

11th International Conference Interdisciplinarity in Engineering, INTER-ENG 2017, 5-6 October
2017, Tirgu-Mures, Romania

Lake Nubia sediment capacity estimation based on satellite remotely sensed detected bathymetry

Mohamed Elsayhaby^a, Omar Makboul^b, Abdelazim Negm^{c,*}

^aPhD student, Civil Engineering Dept., Aswan University, Aswan 81542, Egypt

^bM.Sc. Student, Arab Academy for Science, Technology and Maritime Transport, Alexandria-21913, Egypt

^cProfessor, Department Water and Water Engineering Dept., Faculty of Engineering, Zagazig University, Zagazig, 44519, Egypt

Abstract

This research is concerned with detecting the depths of the Aswan High Dam Lake (AHDL) (particularly Nubia Lake) using Landsat-8 multi-spectral bands with resolution 30m. The method of depths estimating from the satellite images is based on establishing Multiple Linear Regression (MLR) model using logarithms of reflectance bands. Quantifying the error between in-situ measurements and satellite estimated lake depths values. The results indicated that the correlation coefficient ($R = 0.5$) and the Root Mean Square Error (RMSE = 0.6m) for testing data set. The computed depths from the satellite remote sensing data were used to estimate the sediment and erosion capacities in Lake Nubia (LN) since the beginning of the storage process in the lake at the year 1964 till the year 2012. The results are comparable to those of the traditional method (cross section method) and the method of building 3D profile from the field measurements with additional merits of the present approach that it is more flexible and cost-effective tool for bathymetry mapping. Moreover, the results indicated that the computed amount of sediment using the estimated depths from the RS data (the present approach) overestimated the results by 4.16% compared to those computed using the cross-section method adopted by AHDA. On the other hand, the results indicate that the present approach overestimates sediment amount by about 3.93% compared to the results derived from the generated 3D profiles of the Lake based on the field measurements.

© 2018 The Authors. Published by Elsevier B.V.

Peer-review under responsibility of the scientific committee of the 11th International Conference Interdisciplinarity in Engineering.

Keywords: Remote Sensing; Lake Nubia; Multiple Linear Regression; Satellite derived bathymetry; Sediment; Erosion.

* Corresponding author. Tel.: +20-100-573-5345; fax: +20-345-995-20.

E-mail address: amnegg@zu.edu.eg

1. Introduction

Estimating the sediment capacity of the lakes is an essential task for the managers and decision makers of water management sector. Achieving this task based on the field measurements consumes time, money and effort. On the other hand, detecting bathymetric data (depths) using Remote Sensing (RS) data has led to overcome such problems if used in estimating the sediment amount and verified by field measurements. Optical remote sensing offers an alternative to traditional hydrographic surveys for measuring water depth, with the advantage that data are collected synoptically over large areas. By comparison with the traditional method, remote sensing can produce more flexible, efficient and cost effective means of mapping bathymetry. There are several factors affected when measuring depth in shallow water especially rivers such as the degree of transparency of the water, water turbidity, nature of the bottom and the reflection from surrounding area. Remote Sensing (RS) data can be implemented for bathymetry derivation by using two methods: analytical modeling and empirical modeling [1]. In this research, an empirical model is used for bathymetry derivation from Remote Sensing (RS) data. In empirical modeling, the relationships between the remotely sensed radiance or reflectance of a water body and the depth at sampled locations are established empirically without consideration of how the light is transmitted in water [2]. Some researchers try to derive bathymetry using empirical modeling such as [3, 4, 5]. Extensive researches in estimating sediment amount in lakes, using RS and GIS techniques had been investigated in the past four decades. Among of these researches are [6, 7, 8, 9]. The objective of this research is to estimate the sediment capacity of Lake Nubia (LN) (the Sudanese part of Aswan High Dam Lake) till the year 2012 via generating the 3D bed surface of year 2012 from the detected bathymetry data using a Landsat-8 multiband combination and generating the 3D bed surface of year 1964 according to [10].

2. Study Area and Data Collection

2.1. The study area

AHDL is one of the greatest man-made Lakes in the world, created after the construction of the Aswan High Dam (AHD). This Lake extends for 500 km along the Nile River from the southern part of Egypt to the northern part of Sudan. It covers an area of about 6,000 km², of which two-thirds (known as Lake Nasser, 350 km) is in Egypt and one-third (called Lake Nubia, 150 km) is in Sudan [8] as shown in Fig. 1.

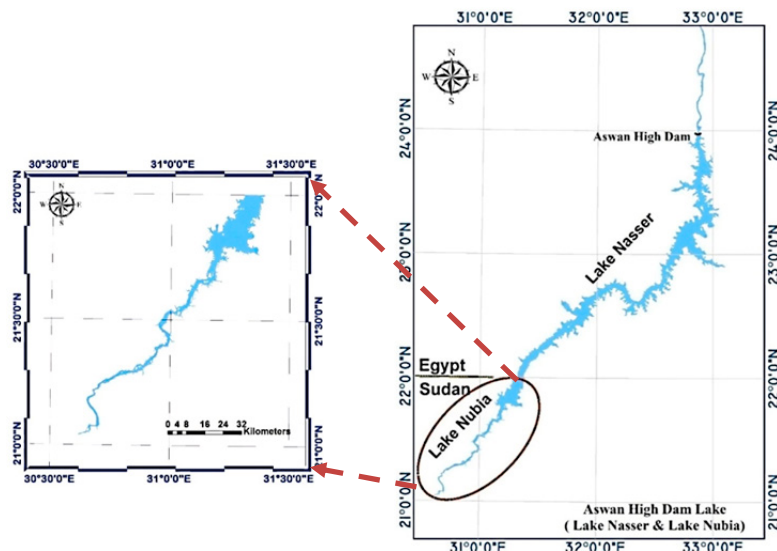


Fig. 1. Location map of the study area within Aswan High Dam Lake.

Lake Nubia, the study area in this paper, is located between latitudes $21^{\circ} 02' 00''$ and $22^{\circ} 00' 00''$ N (upstream the AHD). The southern two thirds of this Lake are narrow, while the remaining northern part is much wider as indicated in Fig. 1.

2.2. Hydrographic survey data

The hydrographic survey data presented by Easting, Northing, and Elevation (E, N, and Z) were used to describe the geometry of Lake Nubia for year 2012. These data were conducted by both AHDA and Nile Research Institute (NRI) using the Odom Hydrographic echo-sounder device (Hydrotrac II) with accuracy up to $0.01\text{m} \pm 0.1\%$ of the measured depth.

2.3. Satellite remote sensing data

Landsat-8 collects image data in 11 spectral bands with a 30 m spatial resolution with (Path/Row = 175/045). The bands used for detecting bathymetry in this study are coastal/ aerosol ($0.435\text{--}0.451\ \mu\text{m}$), blue ($0.452\text{--}0.512\ \mu\text{m}$), green ($0.533\text{--}0.590\ \mu\text{m}$), red ($0.636\text{--}0.673\ \mu\text{m}$) and Near Infrared (NIR) ($0.851\text{--}0.879\ \mu\text{m}$) [11]. The Landsat-8 data used in this study were acquired in 24 May 2013 with an average cloud cover less than 10%. The data were downloaded freely from the earth explorer USGS in level 1 Geotiff (systematic correction) product. These images were geo-referenced by USGS using the world reference system (WGS-84 datum) to Universal Transverse Mercator system (UTM) zone, 36 North projections.

3. Methodology

To achieve the objectives of this study, the following systematic steps which involved in the flowchart shown in Fig.2 were conducted and performed.

3.1. Applying atmospheric correction

The solar radiation passes through the atmosphere before collected by the sensor. Therefore images are affected by several factors such as water vapor and distribution of aerosols (visibility). To correct the atmospheric effect, the radiometric corrected pixel values are firstly converted to spectral reflectance using the gain and bias information of sensor bands from Land-sat metadata file. Then the FLAASH model in ENVI software is used to correct the atmospheric effect. FLAASH normally retrieves aerosol and water vapor information from the image, providing well-adjusted input for the atmospheric correction. FLAASH starts from a standard equation for spectral radiance at a sensor pixel according to Equation 1 [12].

$$L = \left(\frac{Ap}{1 - p_e^s} \right) + \left(\frac{Bp_e}{1 - p_e^s} \right) + L_a \quad (1)$$

where, p is the Pixel surface reflectance, p_e is an average surface reflectance for the pixel and a surrounding region, s is the spherical albedo of the atmosphere and L_a is the radiance back scattered by the atmosphere. A and B are coefficients that depend on atmospheric and geometric conditions but not on the surface. Moreover, A, B, S and L_a are depending on water vapor amount. The input files must contain calibrated radiance values and converted to BSQ or BIP format before the atmospheric correction. In addition to the image file to be corrected, FLAASH also needs information on the geographical centre location of the image and the time it was captured. This information can't be retrieved automatically from the data file, but must be entered by the user. An atmospheric model must be selected depending on climate (latitude and time of year). Urban aerosol model is selected depending on the expected type of aerosols and visibility presence.

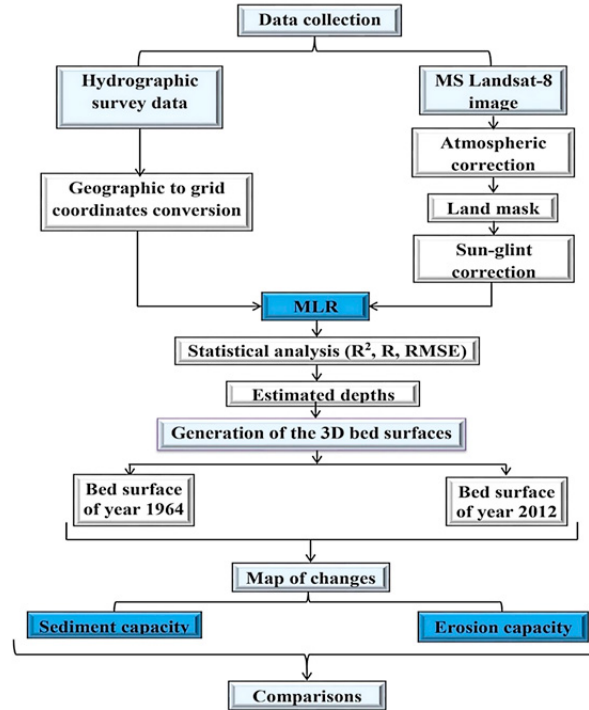


Fig. 2. Flowchart of the procedures adopted in this study for the purpose of estimating sediment and erosion capacities of LN.

3.2. Land masking

When extracting aquatic information, it is useful to eliminate all upland and terrestrial features. Thus, all upland features were masked out of the image. The “land-mask” restricts the spectral range to aquatic features and allows for detailed feature discrimination. Reflectance values of the NIR band were used to prepare the mask which was subsequently applied to all the bands [13]. The threshold value for land/water was calculated to separate water area.

3.3. Applying sun glint correction

Specular reflection of solar radiation, known as sun glint must be removed for accurate benthic habitat classification. The sun glint is corrected by using linear regression of NIR brightness (x-axis) against the visible band brightness (y-axis) [14], this would be homogeneous if not for the presence of sun glint (deep water). The slope of the regression is then used to predict the brightness in the visible band by using Equation 2. The minimum sample size required is two pixels.

$$R'_i = R_i - b_i(R_{NIR} - MIN_{NIR}) \quad (2)$$

where R'_i is the sun glint corrected pixel brightness in band i , b_i is the product of regression slope, R_{NIR} is corresponding pixel value in NIR band and MIN_{NIR} is the min NIR value existing in the sample.

3.4. Multiple linear regression (MLR) model

Multiple linear regression attempts to model the relationship between two or more explanatory variables and a response variable by fitting a linear equation to observed data. Every value of the independent variable x is

associated with a value of the dependent variable y . The regression line for explanatory variables is defined to be as Equation 3.

$$y = \alpha + \beta_1 X_1 + \beta_2 X_2 + \dots + \beta_n X_n \quad (3)$$

Where, α is called the intercept, β_i is called slopes or coefficients and X_n is the reflectance of spectral bands. The main objective in using this technique is to predict the variability the dependent variable based on its covariance with all the independent variables.

3.5. Generation of the 3D bed surfaces maps

The 3D bed surfaces maps for the year 1964 and 2012, generated using the RBF (Radial Basis Function) spatial interpolation method in ArcGIS software [15], were used to create the map of changes through this time period from 1964 to 2012.

3.6. Map of changes derivation

The map of changes, derived by overlaying the two generated bed surfaces maps using ArcGIS Software [15], was produced to estimate the capacity of both sediment and erosion in the study area till the year 2012.

4. Results and Discussions

4.1. The MLR model

The MLR model parameters are obtained as a result of training and testing processes. The input reflectance and in-situ measurement for the model are separated into two parts for training (70%) and for testing (30%). Equation 4 is the deduced equation for estimating depths in this study.

$$Z = -47.73 + 2.37 \times L_C + 5.67 \times L_B + 2.15 \times L_G + 1.25 \times L_R \quad (4)$$

Where, L_C , L_B , L_G and L_R are respectively, the logarithms of the reflectance of coastal, blue, green and red bands. A statistical analysis was performed to compute correlation coefficient (R) and the root mean square error (RMSE in order to evaluate the model performance. The values of R and RMSE are 0.50 and 0.60m respectively for the testing data set. However, for training data set, the MLR has lower performance regarding both R (0.43) and RMSE (1.7m). On the other hand, the observations are supported by establishing a scatter diagram as shown in Fig.3 to compare between the observed depths (field measurements) and the estimated ones. The data scattering presented in Fig.3 shows that the MLR has a reasonable prediction for depths from 20m to 25m (which represents most of the study area) and less performance in predicting depth lower than 20m. Differences in the bottom type misleading the results since the bottom type in the study area are silt, mud and sand.

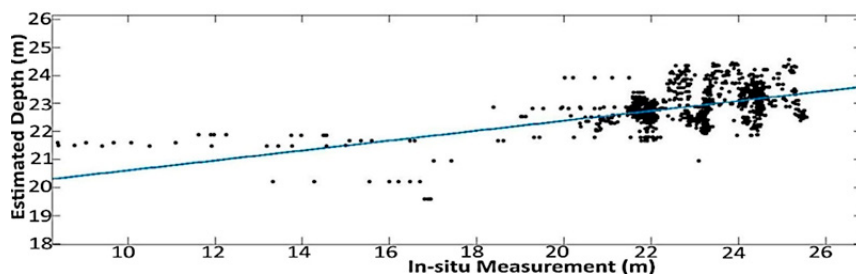


Fig. 3. Comparison between estimated and observed depths of the year 2012.

4.2. The generated bed surface maps

To obtain the complete predict bed surfaces map of the lake by the interpolation process, the Radial Basis function (RBF) method for interpolation is used. Firstly, the predicted (interpolated) bed surface for the year 1964(before dam construction) is generated. For more details about the bed surface generation, especially 1964 bed surface, , interested readers can review [10]. Then the bed surface map of year 2012 is generated, relying on the estimated lake depths from the remotely sensed data, using ArcGIS software. The generated bed surfaces maps are presented in Fig. 4.

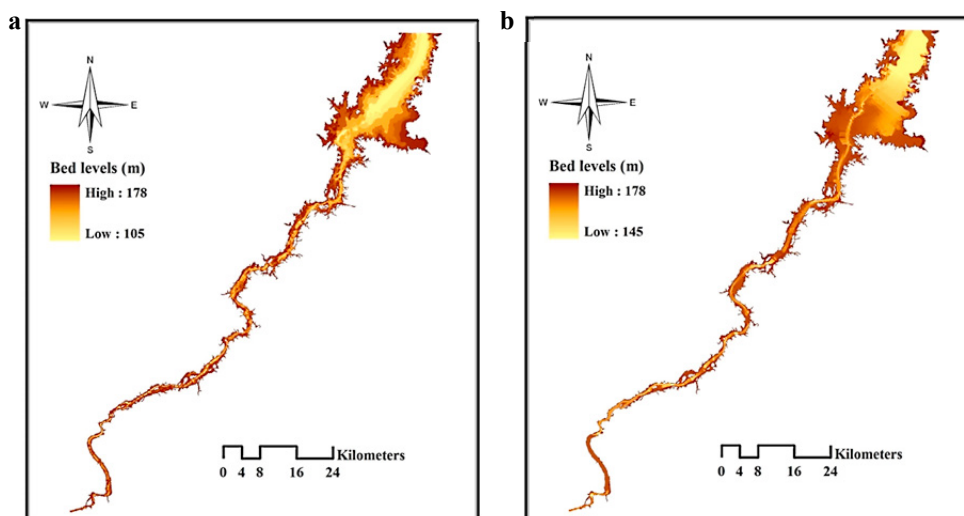


Fig. 4 The generated bed surfaces maps: (a) 1964 bed surface [10]; (b) 2012 bed surface.

4.3. Map of changes

The map of changes for the period (1964-2012) was generated by overlaying the two created bed surfaces, shown in Fig. 4(a) and Fig. 4(b) using ArcGIS software. The map of changes which involves three broad change classes (unchanged, sedimentation and erosion) is presented in Fig. 5.

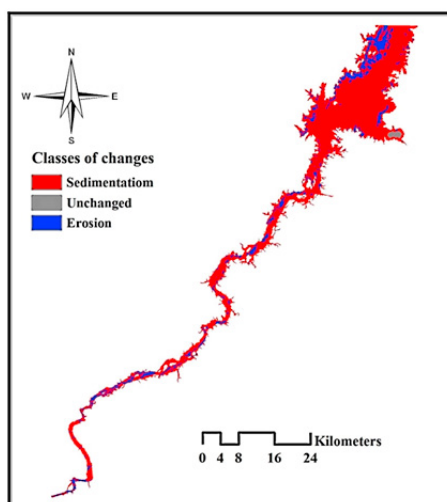


Fig. 5 The produced map of changes for the period (1964-2012).

4.4. Estimation of sediment and erosion

Table 1 shows the sediment and erosion 2D surface areas and amounts in the period (1964 – 2012), which were estimated by using the statistics of the classes of changes in the generated map of changes.

Table 1. Bed changes from the year 1964 to the year 2012.

Bed change	2D area (Km^2)	Amount ($B.m^3$)
Sediment	475.59	6.107
Erosion	79.71	0.304

4.5. Comparisons

The results of using the complimentary cross-section (the traditional method adopted by Aswan High Dam Authority, AHDA) and using the generated 3D profile of the Lake from the field measurements [10] are compared with the present estimated sediment capacity based on the 3D profile of the lake that is built using the predicted depths via multiple linear regression based on the detected bathymetry from the RS satellite data. The cross-section method used by AHDA is taken as reference method when the results are compared.

Table 1 presents a quantitative comparison of the three applied approaches. The computed amount of sediment using the present approach is $6.107 B.m^3$ which is higher than the results of the other two approaches indicating an overestimation by about 4.16% compared the method adopted by AHDA. On the other hand, the results indicate that the present approach overestimates sediment amount by about 3.93% compared to the results derived from the 3D profile of the Lake (which was built based on the field measurements). On the other hand, the difference in the estimation of erosion amounts is small, but the underestimation percentage is almost same as the overestimation percentage in the sediment amount.

Table 2. Quantitative comparison of the estimation using the three approaches till the year 2012.

Bed change category	Estimation by the present approach ($B.m^3$)	Estimation by building 3D profile from the field measurements ($B.m^3$) [10]	Estimation by the cross section method ($B.m^3$) [16]
Sediment	6.107	5.876	5.863
Erosion	0.304	0.315	0.320

Accordingly, the estimated bathymetric data by the applied approach in the present study can be used to estimate the sediment capacity of LN instead of the costly field measurements.

5. Conclusions

This paper presents and discusses the results of estimating Lake Nubia depths and sediment/erosion amount. Results showed that an error of 0.6 m is obtained in depths estimation. This accuracy may be enough when using bathymetry by remote sensing in the preliminary survey. Moreover, the results indicated that the computed amount of sediment using the estimated depths from the RS data (the present approach) overestimated the results by 4.16% compared to those computed using the cross-section method adopted by AHDA. On the other hand, the results indicate that the present approach overestimates sediment amount by about 3.93% compared to the results derived from the generated 3D profiles of the Lake based on the field measurements.

References

- [1] J. Gao, Bathymetric mapping by means of remote sensing: methods, accuracy and limitations. *Progress in Physical Geography*. 33(2009) 103–116.
- [2] G. Doxani, M. Papadopoulou, P. Lafazani, C. Pikridas, M. Tsakiri-Strati, Shallow-Water Bathymetry Over Variable Bottom Types Using Multispectral WorldView-2 Image. *ISPRS - International Archives of the Photogrammetry, Remote Sensing and Spatial Information Sciences*, XXXIX-B8, 2012, pp.159–164.

- [3] Ö. Ceyhan, A. Yalçın, Remote sensing of water depths in shallow waters via artificial neural networks. *Estuarine, Coastal and Shelf Science*. 89(2010) 89–96.
- [4] L. Corucci, Approaching bathymetry estimation from high resolution multispectral satellite images using a neuro-fuzzy technique. *Journal of Applied Remote Sensing*. 5(1) (2011) 053515.
- [5] H. Su, H. Liu, W.D. Heyman, Automated Derivation of Bathymetric Information from Multi-Spectral Satellite Imagery Using a Non-Linear Inversion Model. *Marine Geodesy*. (2008) 281–298.
- [6] S.L. Curzio, F. Russ, M. Caporaso, Application of remote sensing and GIS analysis to detect morphological changes in an artificial lake, *International Journal of Remote Sensing & Geoscience (IJRSG)*. 2(4) (2013) 2319-3484.
- [7] E.A. El-Gammal, Assessment Lake Nasser Egypt within the climatic change. *Journal of American Science*. 6(2010) 305-312.
- [8] A.M. Negm, M. Elsayhaby, K. Ali, A Satellite Remote Sensing Approach to Estimate the Lifetime Span of Aswan High Dam Reservoir. *The Nile River, HdbEnvChem*, DOI: 10.1007/698_2017_15, © Springer International Publishing AG., 2017.
- [9] M.S. El-Sammany, A.M. El-Moustafa, Adaptation of surface water modeling system for sediment transport investigations in Lake Nasser, *Journal of Nile Basin Water Science and Engineering*. 4(1) (2011) 71–85.
- [10] M. Elsayhaby, A. Negm, Building 3D profile for Lake Nubia, <Sudan> using RS/GIS for accurate estimation of Sediment. *Procedia Eng*. 181(2017) 845–852.
- [11] USGS: Department of interior U. S. Geological Survey, Landsat 8 (L8) Data Users Handbook, 2015.
- [12] ENVI, ENVI Atmospheric Correction Module: QUAC and FLAASH User's Guide. ITT Visual Information Solutions, 2009.
- [13] D.R. Mishra, S. Narumalani, D. Rundquist, M. Lawson, Characterizing the Vertical Diffuse Attenuation Coefficient for Downwelling Irradiance in Coastal Waters: Implications for Water Penetration by High Resolution Satellite data. *ISPRS Journal of Photogrammetry and Remote Sensing*. 60(2005) 48–64.
- [14] J.D. Hedley, a. R. Harborne, P.J. Mumby, Simple and Robust Removal of Sun Glint for Mapping Shallow Water Benthos. *International Journal of Remote Sensing*. 26(2005) 2107-2112.
- [15] ESRI: Environmental Systems Research Institute, Help topics of ArcGIS version 9.3 Desktop, Developer center of geographic information systems (GIS) software, Redlands, California, 2008.
- [16] NRI: Nile Research Institute, Annual report of Sedimentation in Lake Nubia –Wadi Halfa Field trips- (1973-2012), National water Research Center, Cairo, Egypt, 2012.